Optics & Laser Technology 49 (2013) 28–32

Contents lists available at SciVerse ScienceDirect

Optics & Laser Technology

journal homepage: www.elsevier.com/locate/optlastec

Research Note

A non-encoding structured light approach with infrared illumination for 3D large field shape measurement

Ye Wang [a], Yan Li [a], Junhong Zhou [a], Jue Zhang [a,b,*], Jing Fang [a,b]

[a] Academy for Advanced Interdisciplinary Studies, Peking University, Beijing 100871, China
[b] College of Engineering, Peking University, Beijing 100871, China

ARTICLE INFO

Article history:
Received 21 October 2012
Received in revised form
28 November 2012
Accepted 9 December 2012

Keywords:
Non-encoding structured light
Infrared illumination system
3D measurement

ABSTRACT

As conventional structured light with temporal and spatial encoded pattern is used to retrieve 3D shape, its measurement accuracy is inevitably affected by the broken and dislocated fringes or grids appearing in shaded, prominent or edge areas. In this study, a non-encoding fringe strategy is presented for large field 3D shape measurement under infrared light illumination. By utilizing the images recorded from several different orientations, the break and dislocation problems can be effectively solved by an algorithm of automatic identification and matching for out-of-plane height curves based on Euclid distance and quaternion. Meanwhile, the field of view can also be enlarged by prolonging the fringes in the edge areas. The examples of retrieving 3D shapes of the statues demonstrate the validation of the proposed approach.

1. Introduction

Various structured light methods [1], mostly with time-multiplexing and spatial codification strategies, have been widely applied to retrieve 3D surface shapes. Among the temporal coding schemes, the binary encoding technique is to be simple and convenient as only two illumination levels are used [1,2]. Because a large number of patterns need to be projected on the surface to form the image series with time sequence, however, the temporal encoding patterns are more suitable for static measurement. To increase acquisition speed for applications to moving object measurement, a variety of spatial encoding structured light schemes have been developed. Phase retrieval techniques has been applied in [3–6] reconstructed 3D surface by using various phase unwrapping algorithms; color in Refs.[7,8] proposed encoded fringe patterns and applied the color information of neighboring stripes to retrieve 3D shape. Nevertheless, a big problem exists in all of those temporal and spatial encoding structured patterns that the shaded, prominent and edge areas on the 3D surfaces lead to the acquired fringes or grids to be broken or dislocated so that there are inevitable errors and even losses of the measurement data [1,9]. In addition, these codification methods are usually affected by noises in various light environments. For the problem resulting from the shadow and tilted areas on surface, Kowarschik et al. [9] proposed a scheme of rotating the object by more than three different angles so that the whole surface could be illuminated with the structured light to complete the lost fringe information in the images with local shadows by those acquired from other orientations. This scheme provided a valuable way to avoid data loss or mistakes so as to reconstruct whole 3D surface from many overlapping views of different directions, even though the phase unwrapping processing was complicated.

In this paper, a novel approach of non-encoding structured light is proposed in capturing images from different directions to reconstruct large field 3D surface. Unlike the sinusoidal patterns used in phase retrieval methods, in the design of the projecting pattern of this study, only two illumination levels, 0 and 1, are used periodically, without any temporal or spatial encoding. As a pattern of binary encoding, it has a variety of advantages such as relatively high spatial resolution, easy segmentation of the viewed patterns and robustness against noise [1,2]. To obtain the height information of a surface as large as possible, the object is illuminated three times from different directions to ensure the fringes with shadow and tilted regions in one of the pictures to be smoothly distributed in the other one. Because the projected pattern is very simple in structure without any coding, the segmentations of those fringes become much easier and more accurate, which thus makes the out-of-plane height curves resulting from different views be easily identifiable. In the combination of the images from neighboring shooting, we propose a correlation algorithm that can correctly match the out-of-plane height curves together with the solution of rotation

* Corresponding author at: Academy for Advanced Interdisciplinary Studies, Peking University, Beijing 100871, China. Tel.: +86 10 62755036; fax: +86 10 62753562.
E-mail address: zhangjue@pku.edu.cn (J. Zhang).

0030-3992/$ - see front matter
http://dx.doi.org/10.1016/j.optlastec.2012.12.008

angles during pattern projections. Moreover, the binary level of fringe intensity used in this projection makes it possible for the pattern illumination using either visible light or infrared source, the latter condition of measurement will be important for night vision applications or in the environments with light noises [10].

2. Material and methods

Fig. 1(a) shows the optical system for surface height measurement. An infrared projector is used to illuminate the specimen with the un-encoded structured pattern in an inclined direction, and an infrared digital camera (computar M1214-MP2, resolution: 2592×1944) is mounted to capture the images in the normal direction to the reference plane. Fig. 1(b) presents the structure of the infrared projector, from left to right: a 3 W infrared light source; a 12.1 in rear Fresnel lens with 220 mm focus; a grating with 0.7 line/mm; a 12.1 in front Fresnel lens with 330 mm focus; and a projecting lens with focus length of 330 mm. In this system, the object under test is placed on a rotating plane, where the rotating axis z is perpendicular to the projection direction.

A nose statue is used as a typical model of shape measurement where the wings of the nose commonly produce image shadows during the front projection on the surface. The fringe patterns captured from three different orientations are shown in Fig. 2(a), (b) and (c), respectively, denoted as the view directions α, β and γ

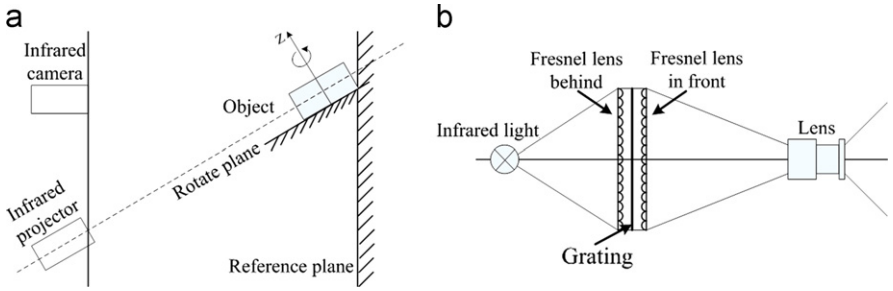

Fig. 1. Schematic illustration of the measurement system with infrared structured light: (a) the optical geometry of projection for triangulation relationship; (b) the infrared projector structure, from left to right: a 3 W infrared light source; a 12.1 in rear Fresnel lens with 220 mm focus; a grating with 0.7 line/mm; a 12.1 in front Fresnel lens with 330 mm focus; and a projecting lens with focus length of 330 mm.

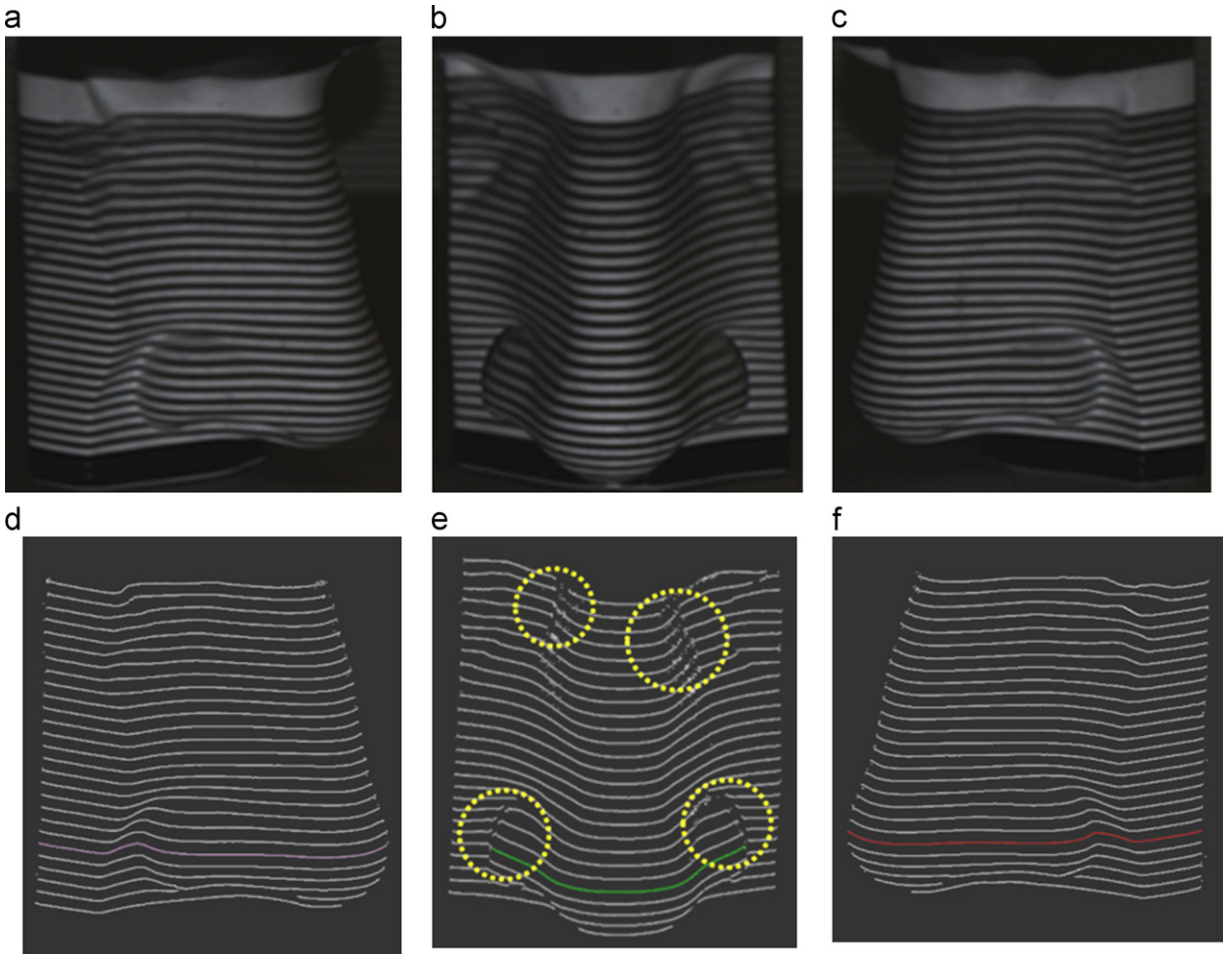

Fig. 2. Pattern pictures captured from the directions of (a) view α; (b) viewβ; (c) view γ; and the corresponding segment results: (d), (e) and (f), where the circles indicate the areas with dislocated fringes due to illumination shadows. (For interpretation of the references to color in this figure legend, the reader is referred to the web version of this article.)

as the object rotated around axis z. The corresponding segmented fringes are shown in Fig. 2(d), (e) and (f), where in Fig. 2(e) corresponding to the image of Fig. 2(b) resulting from normal capturing, the yellow circles point out several broken and dislocated fringes caused by the shaded and prominent parts of the test object, while the fringes in the corresponding regions of Fig. 2(d) and (f), on the other hand, are smoothly connected. By using the information of those easily segmented fringes with respect to neighboring views, a process of five steps with automatic out-of-plane height curves identification and matching is described in the following to reconstruct the wide field 3D surface shape.

1. Detecting the fragmented and dislocated fringes: For any given vertical line, no more than one consecutive part in the fragmented fringe goes through it; thus, only one continuous part in the fragmented fringe will persist. The method developed in Step 4 can detect the dislocated fringes.
2. Using conventional triangulation relationship to calculate the out-of-plane height curves of the corresponding fringes: The out-of-plane height data are needed to obtain rotation matrix and final reconstruction. For convenience, each out-of-plane height curve is marked by a unique serial number; for instance, the first curves in the views of α, β and γ are represented as the curves α_1, β_1 and $\gamma_1$respectively. Because the acquired infrared fringes are neither spatial nor temporal encoded, we just need to identify which two curves in the neighbor shooting angles are matched to each other in an alternative way. Based on the truth that there exists an overlapping segment in the out-of-plane height curves among different views, the segment is used to recognize the corresponding matched curves. Without loss of generality, we choose k points (for instance, $k=300$) in the overlapped segment for matching calculation.
3. Calculating the rotation matrix between two curves from neighboring images. The first curve is represented as $C_1=[x_{11}\cdots x_{1k};\ y_{11}\cdots y_{1k};\ 1\cdots 1]$, and the second curve is $C_2=[x_{21}\cdots x_{2k};\ y_{21}\cdots y_{2k};\ 1\cdots 1]$, where k is the number of the point in each part of curve. The centroid of the ith curve is $(\bar{x}_i,\bar{y}_i)=\left((1/k)\left(\sum_{i=1}^{k}x_i\right),(1/k)\left(\sum_{i=1}^{k}y_i\right)\right)$, where $i=1, 2$. By adding the coordinate difference$(\Delta x,\Delta y)=(\bar{x}_1-\bar{x}_2,\bar{y}_1-\bar{y}_2)$to the second curve, the two curves can be translated to the same centroid, and the second curve after translation is denoted as $C_t=[x_{t1}\cdots x_{tk};\ y_{t1}\cdots y_{tk};\ 1\cdots 1]$. In our study, the quaternion in [11] is applied to estimate the rotation matrix among different views; thus, the orthogonal rotation matrix R is obtained by $R=M(M^{T}M)^{-1/2}$, where$M=C_1\,C_t^{T}$, ensuring that the curve C_t has no deformation in further rotation procedure.
4. Identifying and matching the out-of-plane height curves: The matched curve is explored at neighbor shooting angle in certain ranges by traversal of the same length curves and solving the rotation matrix. For those patterns shown in Fig. 2, the curves γ_2–γ_6 in Fig. 2(f) are chosen as the candidates. Take curve γ_2 and β_4 for instance; after translating and rotating the two curves, the total Euclid distance of all corresponding points in two possible overlapped curves is $d=\sum\sqrt{(x_{1i}-x_{ti})^2+\left(y_{1i}-y_{ti}\right)^2}$. By calculating d between all curves with k points in length in the curves γ_2–γ_6 and the overlapped segment in the curve β_4, there must exist a part of curve in the view γ for which d reaches the minimum value. Generally, the overlaps on the dislocated out-of-plane height curves do not really exist on the test object; thus the value of d between the curves generated by dislocated fringes and overlapped segment is always very large. Therefore, those dislocated fringes can be easily detected and then eliminated in further matching computations. In this example, the curve γ_4 is proved to match with curve β_4, and the displacements of the centroid coordinate of curve β_4 before and after rotation are the translation parts of the rotation and translation matrix. Fig. 3 presents a typical matching result based on the curve identification and matching mentioned above. The pink line, the green line and the red line in Fig. 3 show the acceptable matching result of three typical out-of-plane height curves α_4, β_4 and γ_4, which correspond to the colorful lines in Fig. 2(d), (e) and (f), respectively.
5. Matching all out-of-plane height curves in different views into a unique coordinate system: The rotation and translation matrix between view α and view β is denoted as R_{12}, and the matrix between view β and view γ is denoted as R_{23}. Because there are overlaps between view α and view γ, all curves in the view α can match with all curves in the view γ on multiplying $R=R_{12}R_{23}$. In this way, 3D reconstruction of the object surface is realized.

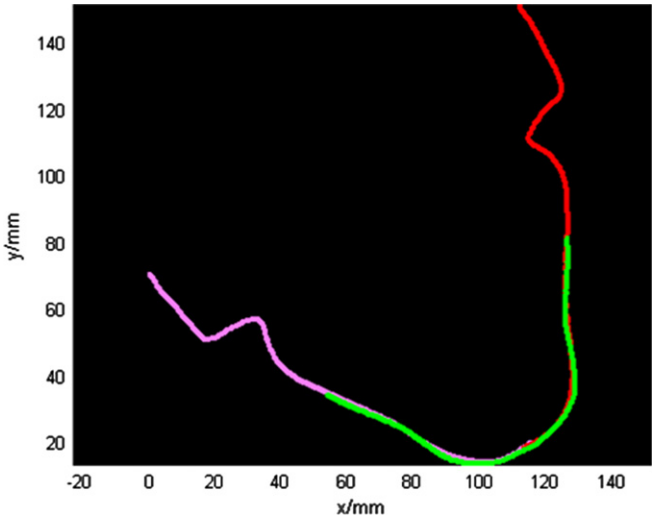

Fig. 3. A curve identification and matching result. The colorful lines are out-of-plane curves from three projected directions: the green one is α_4, the red one is β_4 and the blue one is γ_4. The colorful lines are transferred by the lines in Fig. 2 by using triangulation relationship. (For interpretation of the references to color in this figure legend, the reader is referred to the web version of this article.)

3. Results

To prove the efficiency of the proposed method, the 3D reconstruction results of two statues are presented in Figs. 4 and 5. There exist overlaps between view α and view γ, so only two captured directions are presented in Figs. 4(a) and 5(b). Fig. 4(a) shows the 3D height points of the nose statue viewed in three different orientations, where the red area is obtained from the view α and the blue area is acquired from the view γ. The included angle between view α and view β is 53°, and the intersection angle between view β and view γ is 60°. Fig. 4(b) gives the 3D surface reconstruction of the nose corresponding to Fig. 4(a). For further demonstration, similar processing is carried out for a face statue as shown in Fig. 5, where (a) gives the fringe patterns captured from three different views, (b) shows the 3D height points of the identified curves with matching from neighboring images of shooting, and (c) presents the reconstructed results of the face surface. The included angle

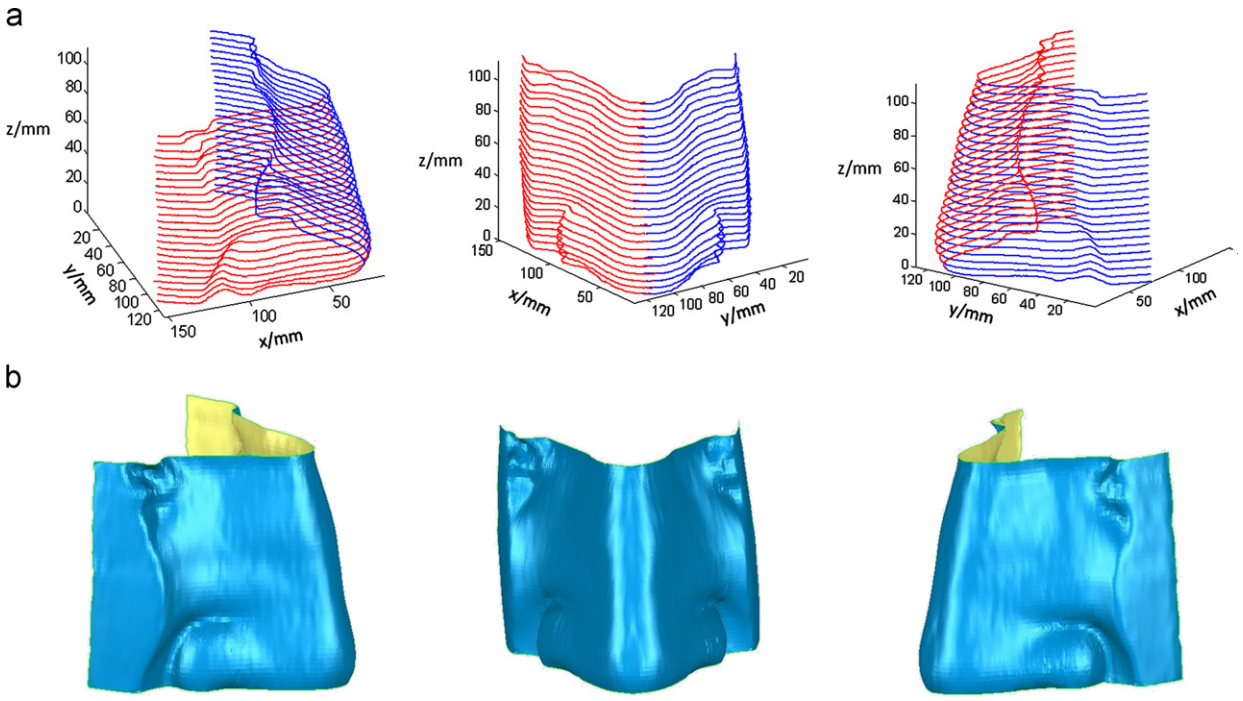

Fig. 4. (a) 3D points of a nose statue resulting from identifying and matching of height curves from different orientations, with the red part corresponding to the view α and the blue part to the view γ and (b) reconstructed 3D shapes shown in different views with the view angle of 290°. (For interpretation of the references to color in this figure legend, the reader is referred to the web version of this article.)

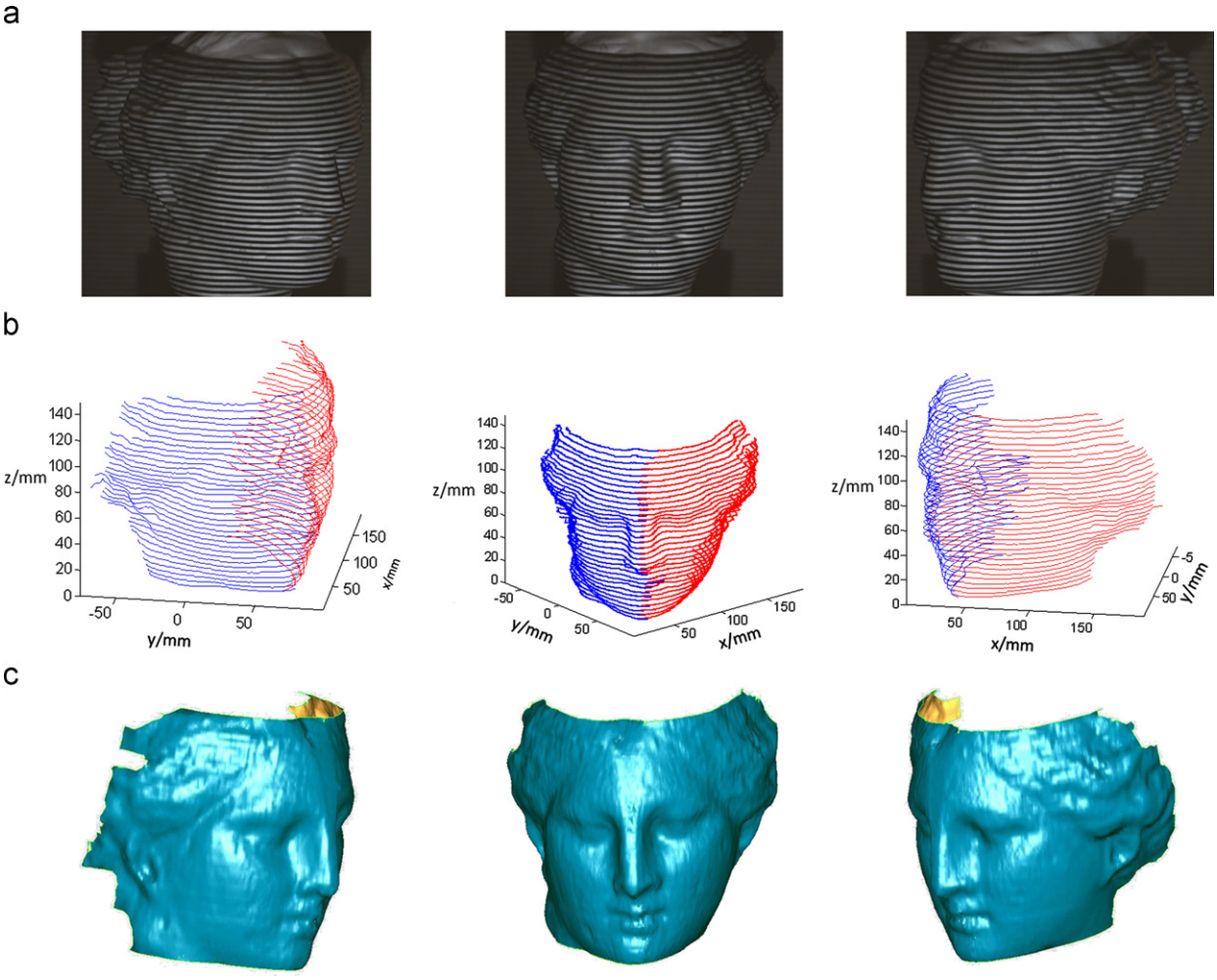

Fig. 5. (a) Fringe images of a face statue shot from three directions; (b) 3D points of the face statue resulting from identification and matching processing, with the red part corresponding to the view α and the blue part to the view γ; and (c) 3D reconstruction result of the face statue with a view angle of 260°. (For interpretation of the references to color in this figure legend, the reader is referred to the web version of this article.)

between view α and view β is 33°, and the intersection angle between view β and view γ is 42°.

In this experiment, the distance between the reference plane and infrared camera is 1.2 m, and the distance between infrared camera and infrared projector is 30 cm. In addition, the angle between the projecting and the receiving directions is 26°. With this system layout, the accuracy is around 0.5 mm in height measurement. In fact, the visual angle can be enlarged to 290°. Because only the distortion of central lines of fringes are recorded and used for out-of-plane height calculation, the accuracy of this method is relatively lower than those of the techniques in [3–6], but the non-encoding structured light approach can reduce information loss caused by shadow and prominent parts, thus making the measurement less sensitive to noise. Full-field measurement would be retrieved by adding the number of projected directions to four or more.

4. Conclusion

In conclusion, the non-encoding of the structured light allows the projected fringes easily segmented to produce the out-of-plane height curves and correctly matched for those captured from different views to eliminate the errors of measurement in the shaded, prominent areas caused by projection. Consequently, the range of the measured surface can be enlarged to 290° by extending these non-encoding fringes to the edge areas under multiple views. Moreover, based on those infrared structured fringes, the presented approach is less sensitive to light environments and could provide night viewing measurement. Further studies will focus on dynamic measurement of full-field 3D shape using multiple cameras from different views.

References

[1] Salvi J, Armangue X, Batlle J. Pattern codification strategies in structured light systems. Pattern Recognition 2004;37:827–49.
[2] Geng J. Structured-light 3D surface imaging: a tutorial. Advances in Optics and Photonics 2011;3(2):128–60.
[3] Windecker R, Franz S, Tiziani HJ. Optical roughness measurement with fringe projection. Applied Optics 1999;38:2837–42.
[4] Dursun A, Ozder S, Ecevit FN. Continuous wavelet transform analysis of projected fringe patterns. Measurement Science and Technology 2004;15:1768–72.
[5] Zhong J, Weng J. Phase retrieval of optical fringe patterns from the ridge of a wavelet transform. Optics Letters 2005;30:2560–2.
[6] Quan C, Chen W, Tay CJ. Phase-retrieval techniques in fringe-projection profilometry. Optics and Lasers in Engineering 2010;48:235–43.
[7] Zhang L, Curless B, and Seitz SM. Rapid shape acquisition using color structured light and multi-pass dynamic programming. In: Proceedings of the first IEEE international symposium on 3D data processing, visualization, and transmission, 2002. p. 24–36.
[8] Chen HJ, Zhang J, Fang J. Surface height retrieval based on fringe shifting of color-encoded structured light pattern,. Optics Letters 2008;33:1081–3.
[9] Kowarschik R, Kuhmstedt P, Gerber J, Schreiber W, Notni G. Adaptive optical three-dimensional measurement with structured light,. Optical Engineering 2000;39(1):150–8.
[10] Frueh C and Zakhor A, Capturing 2½D depth and texture of time-varying scenes using structured infrared light, In: Proceedings of the fifth international conference on 3-D digital imaging and modeling, 2005. p. 318–25.
[11] Horn B, Hilden H, Negahdaripour S. Closed-form solution of absolute orientation using orthonormal matrices. Journal of the Optical Society of America A 1988;5(7):1127–35.